

Theoretical band-structure spectroscopy of $\text{Au}_x\text{Pd}_{1-x}$ alloys

P. Weinberger and L. Szunyogh*

Institut für Technische Elektrochemie, Technische Universität Wien, Getreidemarkt 9/158, A-1060 Wien, Austria

B. I. Bennett

Los Alamos National Laboratory, Los Alamos, New Mexico 87545

(Received 20 August 1992)

Based on electronic structure calculations in terms of the all-electron self-consistent-field fully relativistic Korringa-Kohn-Rostoker coherent potential approximation for $\text{Au}_x\text{Pd}_{1-x}$, the ultraviolet photoelectron, the Au $N_{6,7}$ x-ray emission, as well as the Au $N_{6,7}$ valence-valence (VV) and the Pd $M_{4,5}$ VV Auger electron intensities are calculated for a wide range of concentrations by using the fully relativistic approaches for the corresponding cross sections. The variation of the line shapes for these spectra can be explained mostly by the changes of the valence d band with the concentration. Good quantitative agreement with available experiments is found.

I. INTRODUCTION

Due to its important catalytic properties the $\text{Au}_x\text{Pd}_{1-x}$ system, which forms a solid solution for the whole range of x , has become subject of extended experimental investigations that focus on surface properties like segregation, diffusion, etc. From both the experimental and the theoretical point of view the existence of a strong interaction between the Au $5d$ and Pd $4d$ band also raises an interest in the bulk electronic properties. Experimentally, valence-band spectroscopies like photoelectron spectroscopy (PES) and x-ray emission spectroscopy (XES) provide direct mappings of the (bulk) electronic structure.^{1,2} Concomitantly, electronic structure calculations, in terms of the local-density approximation (LDA), using different computational techniques have been reported for dilute solutions³ and for some selected compositions of this series.^{2,4-6} To date, no systematic theoretical study of the electronic structure and the spectroscopical properties of the entire system has been published. In this work we present over the entire concentration range of $\text{Au}_x\text{Pd}_{1-x}$, in terms of the self-consistent-field relativistic Korringa-Kohn-Rostoker coherent potential approximation (SCF-RKKR-CPA) method,⁷ and using a fully relativistic formulation for the transition matrix elements, a comprehensive study of the theoretical spectroscopy for this system.

II. THEORY

The concept of theoretical valence-band spectroscopy is based on the interpretation of excitation spectra in terms of the ground-state electronic structure. This implies that the influence of electron correlation is neglected beyond the level of LDA. This approach, however, provides a clear and transparent interpretation of the spectroscopical intensities. Due to the overall similar approximations made,⁸ the PES, XES and core-valence (CCV) AES can be generally written as

the sum of weighted partial densities of states (PDOS's) (Refs. 9-11):

$$I^\alpha(E) = \sum_{\kappa} \sigma_{\kappa}^\alpha(E) n_{\kappa}^\alpha(E) , \quad (1)$$

where the $\sigma_{\kappa}^\alpha(E)$ are the κ -like partial cross sections and $n_{\kappa}^\alpha(E)$ denotes the κ -like PDOS for the alloy species α . The core-valence-valence (CVV) AES intensity is given by the convolution of PDOS's (Ref. 11) with the associated cross sections:

$$I^\alpha(E) = \sum_{\kappa\kappa'} \int dE' \sigma_{\kappa\kappa'}^\alpha(E, E') n_{\kappa}^\alpha(E-E') n_{\kappa'}^\alpha(E') . \quad (2)$$

For PES these componentlike intensities are combined, as weighted by the species concentrations, to give

$$I(E) = \sum_{\alpha=A,B} c_{\alpha} I^{\alpha}(E) . \quad (3)$$

For XES and AES, the intensities associated with core states on the same atomiclike shell are superposed according to the corresponding spin-orbit splitting. Due to the finite lifetime of valence and core holes, the intensities are convoluted by Lorentzian functions, as well as by a Gaussian in order to mimic the finite spectrometer resolution. For the XES and AES spectra, the half widths of these functions were chosen to be the same as in Ref. 11, while in the case of ultraviolet photoemission spectroscopy (UPS) we used a half width of 0.7 eV for the spectrometer resolution.

III. RESULTS AND DISCUSSION

A. Densities of states

According to Eqs. (1) and (2) the theoretical spectra are interpreted as a mapping of the PDOS's. Before presenting and discussing the calculated spectra it is useful to show the d -like PDOS's for both the Au and the

Pd components for some of the investigated compositions (Fig. 1). The main characteristics of the Au $5d$ - Pd $4d$ band can be briefly summarized as follows: (i) The peak in the Au $d_{3/2}$ states is located near an energy around -6 eV with respect to the Fermi level (ϵ_F) and moves slightly to lower energies becoming narrower as the concentration of Au decreases. This produces a virtual bound-state (VBS)-like feature for the dilute Au case. (ii) The Au $d_{5/2}$ states are governed by a much stronger interaction with the Pd d -like (mostly $d_{3/2}$) states. For the dilute Pd case these states are situated predominantly between -5 eV and -1 eV, while with increasing Pd content this structure spreads out and its maximum will be shifted below -5 eV for the dilute Au case. (iii) Due to the considerably smaller spin-orbit splitting, the Pd d -like states are less separated than those related to Au. The VBS-like double peak, located between -2 eV and -1 eV for the Au-rich system, becomes well separated and both move continuously towards higher energies as the Pd concentration increases. At high Pd concentration, the d -like states give rise to two sharp peaks, one at -1 eV below ϵ_F and another at ϵ_F .

B. Photoelectron spectra

The results for the UPS intensities (He II line) of the $\text{Au}_x\text{Pd}_{1-x}$ system are shown in Fig. 2(a). All features of these spectra in the entire energy and concentration range can be interpreted in terms of the PDOS's, whose

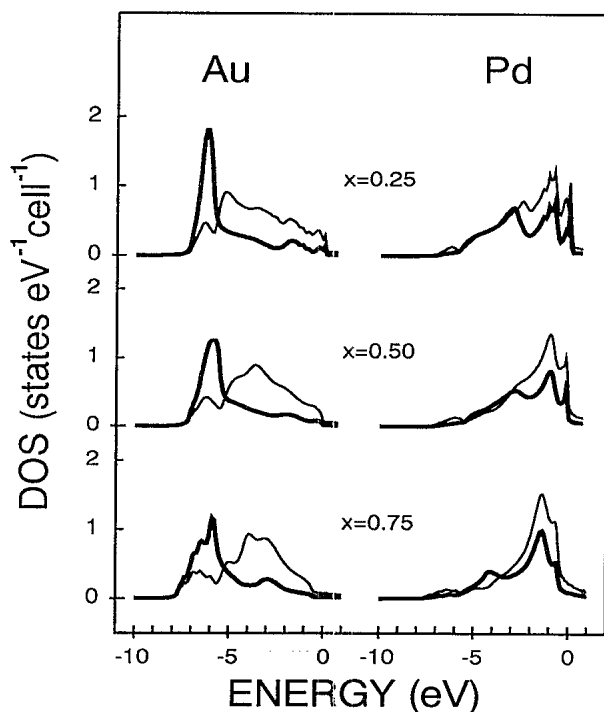


FIG. 1. Local partial d -like densities of states for Au and Pd in $\text{Au}_x\text{Pd}_{1-x}$ for $x = 0.25, 0.50,$ and 0.75 (Ref. 7). The thick and thin solid lines depict the $d_{3/2}$ and the $d_{5/2}$ states, respectively. The zero of the energy scale refers to the Fermi level for each composition.

characteristics have been discussed in the preceding section. For illustration, the componentlike contributions to the intensity are also presented for some compositions in Fig. 2(b). It is clear, for the case of $x = 0.9$ the spectrum is dominated by the Au contribution and for the case of $x = 0.2$ by that of Pd. For $x = 0.6$ both constituents have approximately equal contributions to the spectrum. For $x = 0.9$ the two main peaks at about -6 eV and -3 eV come mostly from the Au $d_{3/2}$ and $d_{5/2}$ states, respectively, and the contribution related to Pd shows up only as a shoulder at -1.5 eV. For $x = 0.2$ the peaks at -3 eV and -1 eV are attributed mainly to Pd states with a small contribution from the Au $d_{5/2}$ states. The small peak below -6 eV has predominantly Au character (see Fig. 1).

Experimental results relevant for comparison are found in Ref. 1. The authors show their spectra including the background intensity. The experimental spectra are in reasonable agreement with the theoretical results in all of the peak positions and peak shapes. A quantitative comparison can be made by comparing the binding energies.¹ In Fig. 3 these energies are shown for both, the experiment and the present calculation. The trends in the binding energies are very well reproduced by the theoretical calculations with the exception that the position

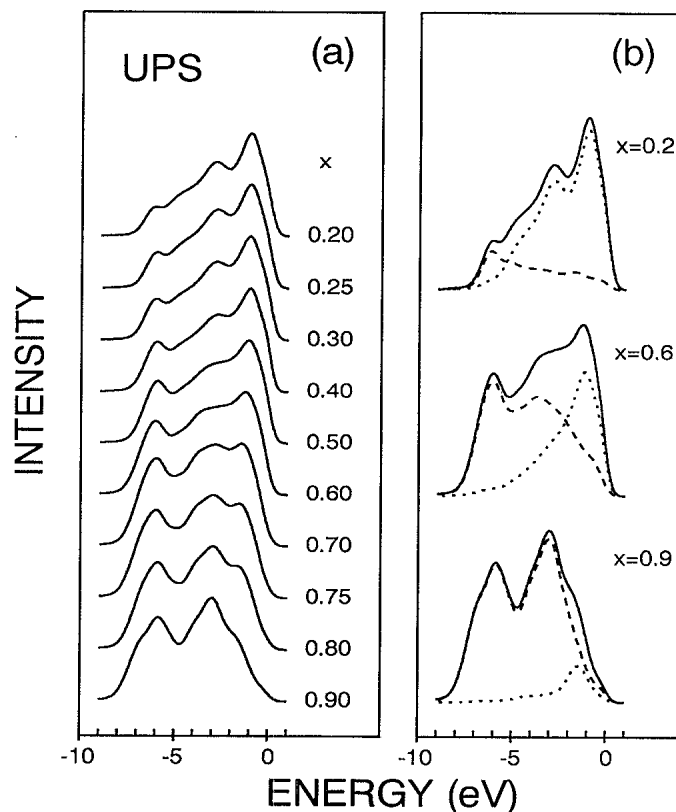


FIG. 2. (a) Calculated UPS intensities ($h\nu=40.81$ eV) for $\text{Au}_x\text{Pd}_{1-x}$ and (b) its resolution into componentlike contributions for the cases $x = 0.2, 0.6,$ and 0.9 (solid line: total spectrum; dashed: Au; dotted: Pd). The highest possible kinetic energy for the emitted electrons coincides with the zero of the energy scale for each case.

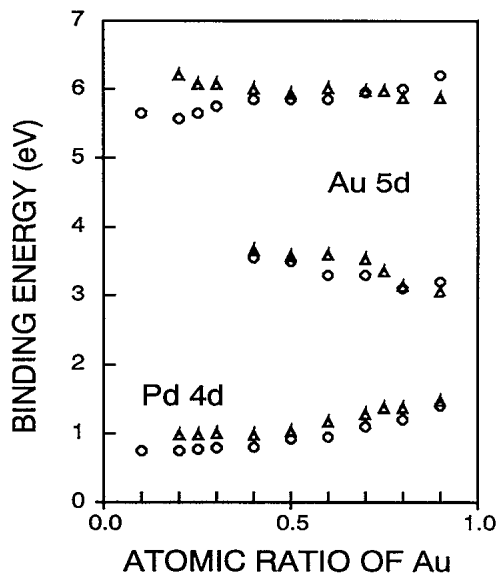


FIG. 3. Binding energies for Au 5d and Pd 4d bands in $\text{Au}_x\text{Pd}_{1-x}$ deduced from measured UPS intensities (Ref. 1) (open circles) and from present calculation (triangles).

of the Au $5d_{3/2}$ band from the theory decreases with Au concentration, while the experiment shows it increasing. This disagreement applies to Au contents below $x = 0.4$. The theoretical Au $5d_{5/2}$ and Pd 4d binding energies deviate from the experimental ones by less than 0.3 eV. In general, the comparison between the experimental and the theoretical binding energies supports the assumption of the single electron picture for this alloy.

C. Soft x-ray emission spectra

Experimental and theoretical Au $N_{6,7}$ soft x-ray emission spectra for some compositions of the Au-rich system have been presented in Ref. 2. In these spectra the intensities of two different transitions, namely, that coming from the $4f_{5/2}$ (N_6) and that from the $4f_{7/2}$ (N_7) core holes, are superposed. Theoretically, the difference of these two core levels ($\Delta\epsilon_C$) is about 3.8 eV, however, since the core holes can be screened differently, the effective energy shift between the two types of spectra can deviate from this value. Therefore we treated $\Delta\epsilon_C$ as an adjustable parameter. For the experimental spectrum in the dilute Pd system the main peak (at 6 eV below the top of the spectrum) and the shoulder to the left of this peak are separated by about 1 eV.² In order to get this separation for the case of $x = 0.9$ we fitted 3 eV for $\Delta\epsilon_C$ and we used this value for all the other concentrations. The corresponding results are shown in Fig. 4(a). As

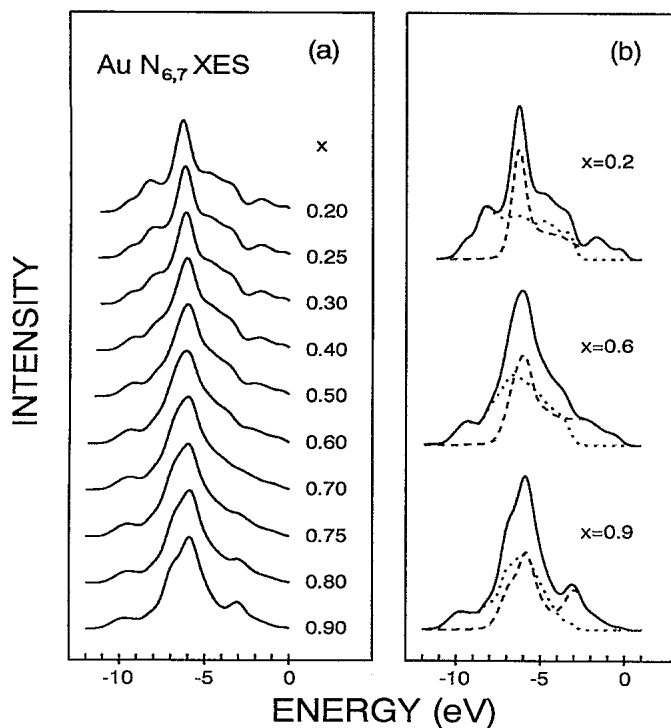


FIG. 4. (a) Theoretical Au $N_{6,7}$ XES intensities in $\text{Au}_x\text{Pd}_{1-x}$. In part (b) the N_6 (dashed) and the N_7 (dotted) contributions are also shown for the cases $x = 0.2, 0.6,$ and 0.9 , whereas the total spectra are displayed by solid lines. The maximum energy of the emitted radiation corresponds to the zero of the energy scale.

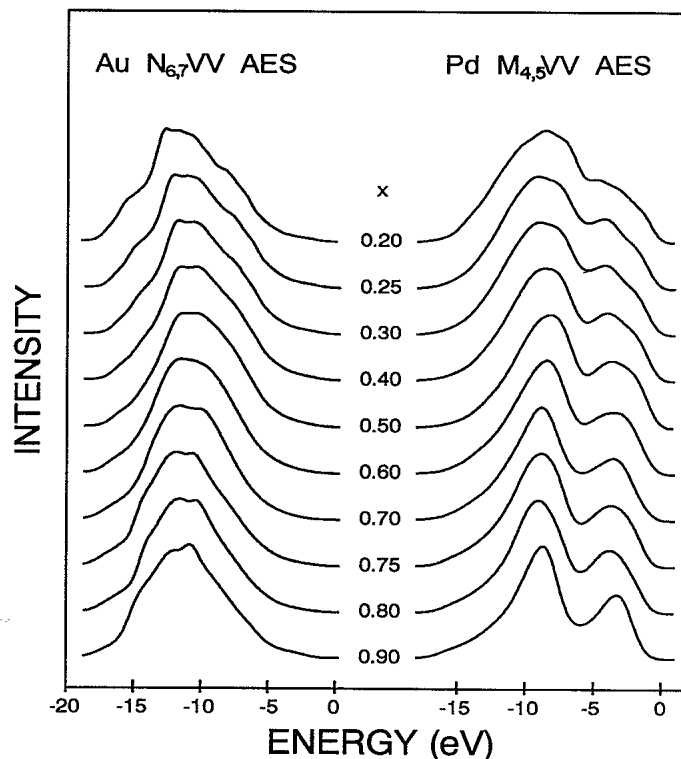


FIG. 5. Calculated Au $N_{6,7}$ VV and Pd $M_{4,5}$ VV Auger electron spectra in $\text{Au}_x\text{Pd}_{1-x}$. The maximum kinetic energy of the Auger electrons corresponds to the zero of the energy scale.

pointed out in Ref. 2, due to the dipole selection rules, the $5d_{3/2}$ states contribute merely to the N_6 transition, while the $5d_{5/2}$ states contribute to both. Nevertheless, it should be noted that these states have a relatively small contribution (less than 10% for all compositions) to the N_6 transition. Therefore the resolution of the theoretical spectra into their N_6 and N_7 components, which is shown for $x = 0.2, 0.6,$ and 0.9 in Fig. 4(b), is practically reduced to a resolution into partial contributions arising from Au $5d_{3/2}$ and $5d_{5/2}$ states, respectively. The typical changes in Fig. 4(a) can therefore be again traced in terms of the PDOS's in Fig. 1. An induced peak at about -2 eV arises with increasing Pd content due to the hybridization between Au and Pd states, which clearly shows that the Au d band cannot be regarded to be "atomiclike" even for the dilute Au case.

D. Auger electron spectra

As also indicated by Eq. (2), the interpretation of the CVV AES is less straightforward. In addition, the Auger process is known to be influenced by correlation (both initial and final states) effects, which in several cases allows merely a qualitative interpretation of these spectra in terms of the single electron picture.¹¹ Nevertheless, because of its simplicity, band-structure spectroscopy facilitates the study of alloying effects also in this case. This is clearly seen from Fig. 5. The rather broad Au N_6 VV and N_7 VV AES peaks strongly overlap. This has been already stressed in context with the $N_{6,7}O_{4,5}O_{4,5}$ spectrum of the pure Au metal.^{12,13} Indeed, the theoretical spectrum for the dilute Pd case ($x = 0.9$) displays

the main characteristics of the pure Au spectrum, i.e., a smaller peak left to the main peak of the spectrum, attributed to the maxima of the two component spectra. Of course, the low-energy satellite profile in the experimental spectrum, associated with a deep bounded component ($1S_0$) of the final state multiplet^{12,13} is not reflected in the present LDA spectrum. The formation of the VBS-like peak below -6 eV in the Au $d_{3/2}$ PDOS shows up obviously with increasing Pd content in a corresponding shift of the maximum of the spectrum from -11.1 eV at $x = 0.9$ to -12.7 eV for $x = 0.2$.

Because of the larger (~ 5.6 eV) energy difference between the Pd $3d_{3/2}$ (M_4) and $3d_{5/2}$ (M_5) core levels and the fairly narrower single spectra, the two contributions are rather separated in the Pd $M_{4,5}$ VV AES and result in two main peaks for the dilute Pd system. When the Pd content increases, due to the broadening of the Pd VBS-like peak, the two contributions overlap increasingly, and for the dilute Au case merely a shoulder to the right of the main peak can be observed, which is a well-known feature also for the pure Pd spectrum.^{11,14}

In summary we can state that based on a precise electronic structure calculation the alloying effects seen in the different spectra of the Au_xPd_{1-x} system can be analyzed in terms of the relativistic band-structure spectroscopy in the framework of the single electron picture.

ACKNOWLEDGMENTS

The authors are indebted to the financial support of the Austrian Science Foundation (P7996) and of the Austrian Ministry of Science (Zl. 49.731/2-24/91).

*On leave from Physical Institute, Technical University Budapest, Budafoki út.8, H-1111 Budapest, Hungary.

¹J.A. Nicholson, J.D. Riley, R.C.G. Leckey, J.G. Jenkin, and J. Liesegang, *J. Electron Spectrosc. Relat. Phenom.* **15**, 95 (1979).

²P. Weinberger, J. Kudrnovský, J. Redinger, B.I. Bennett, and A.M. Boring (unpublished).

³M.G. Ramsey and P.V. Smith, *J. Phys. F* **12**, 1697 (1982).

⁴J. Kudrnovský, V. Drchal, and J. Mašek, *Phys. Rev. B* **35**, 2487 (1987); J. Kudrnovský and V. Drchal, *Phys. Status Solidi B* **148**, K23 (1988).

⁵P. Weinberger, R. Dirl, A.M. Boring, A. Gonis, and A.J. Freeman, *Phys. Rev. B* **37**, 1383 (1988).

⁶E. Arola, C.J. Barnes, R.S. Rao, and A. Bansil, *Phys. Rev. B* **42**, 8820 (1990).

⁷P. Weinberger, J. Kudrnovský, J. Redinger, B.I. Bennett,

and A.M. Boring (unpublished).

⁸P. Weinberger, *Electron Scattering Theory for Ordered and Disordered Matter* (Clarendon, Oxford, 1990).

⁹J. Staunton, B.L. Györfy, and P. Weinberger, *J. Phys. F* **10**, 2665 (1980).

¹⁰P. Marksteiner, P. Weinberger, R.C. Albers, A.M. Boring, and G. Schadler, *Phys. Rev. B* **34**, 6730 (1986).

¹¹L. Szunyogh, P. Weinberger, and J. Redinger, *Phys. Rev. B* **46**, 2015 (1992).

¹²R. Nyholm, K. Helenelund, B. Johansson, and S.-E. Hörnström, *Phys. Rev. B* **34**, 675 (1986).

¹³J.A. Evans, A.D. Laine, P.S. Fowles, L. Duò, J.F. McGilp, G. Mondio, D. Norman, and P. Weightman, *J. Phys. C* **2**, 195 (1990).

¹⁴P. Weightman and P.T. Andrews, *J. Phys. C* **13**, L815 (1980).